

Virological Analysis in Patients with Human Herpes Virus 6–Associated Ocular Inflammatory Disorders

Sunao Sugita,^{1,2} Norio Shimizu,³ Ken Watanabe,³ Manabu Ogawa,² Kazuichi Maruyama,⁴ Norio Usui,⁵ and Manabu Mochizuki²

PURPOSE. To determine whether human herpes virus 6 (HHV-6) genomic DNA and mRNA can be detected in ocular samples from patients with inflammatory disorders, and whether viral replication is involved in the development of inflammation in the eye.

METHODS. After informed consent was obtained, ocular fluid samples (aqueous humor and vitreous fluids) were collected from 350 patients with uveitis or endophthalmitis. Corneal samples were also collected from 65 patients with corneal infections. Multiplex PCR was performed to screen ocular samples from the patients for HHV-1 to HHV-8. Samples were also assayed for HHV-6 DNA using quantitative real-time PCR. Primers for nested RT-PCR were designed to detect amplification of mRNA (HHV-6 A IE1 U90).

RESULTS. PCR results indicated a total of seven patients with uveitis or endophthalmitis (7/350, 2%+) and a single patient with corneal inflammatory disease were positive for HHV-6 DNA (1/65, 1.5%+). These eight patients had high copy numbers of HHV-6 DNA, with values ranging from 4.0×10^3 to 5.1×10^6 copies/mL. Real-time PCR analysis indicated that two of these cases were HHV-6 variant A and six cases were variant B. In addition, HHV-6 mRNA was clearly detected in vitreous cells collected from one of the patients, suggesting that viral replication may occur in the eye.

CONCLUSIONS. Our results indicate that HHV-6 infection/reactivation is implicated in ocular inflammatory diseases. (www.umin.ac.jp/ctr/index/htm number, R000002708.) (*Invest Ophthalmol Vis Sci.* 2012;53:4692–4698) DOI:10.1167/iov.12-10095

Human herpesvirus 6 (HHV-6) is the causative agent of Hexanthera subitum in children and has been associated with a number of inflammatory and neurological disorders

worldwide. It has been implicated in hepatitis, pneumonitis, and severe infections of the central nervous system in both immunosuppressed and immunocompetent patients. HHV-6 can reactivate from its latent form after primary infection. In the case of eye diseases, it has been implicated in AIDS-associated retinitis,^{1–3} uveitis,^{4–8} corneal inflammation,⁹ and optic neuropathy.^{10–12} Two variants of HHV-6 have been identified. HHV-6A is less often associated with disease and has a greater predilection for neural cells than HHV-6B.¹³ Although HHV-6A DNA is frequently found in the nervous system of infected adults, HHV-6B DNA is rarely present in ocular fluids, although it is found in most documented primary HHV-6 infections.

Diagnosis of clinically relevant HHV-6 can be challenging due to the high prevalence of infection and viral persistence. Detection of viral nucleic acids may indicate active or latent infections, depending on the clinical setting and specimens tested. Quantitative PCR methods have been established to detect active infections. Detection of HHV-6 DNA in plasma or serum is indicative of active replication and is therefore more directly interpretable.^{14,15} Using these PCR techniques, several investigators previously reported that HHV-6 genomic DNA is found in ocular inflammatory diseases, including infectious uveitis and endophthalmitis^{1–8}; however, involvement of HHV-6 in ocular infections has not yet been clearly demonstrated.

Therefore, we designed experiments to investigate whether ocular samples from patients with various ocular inflammatory disorders contain HHV-6 genomic DNA, whether ocular samples from noninflammatory patients also contain HHV-6 DNA, whether positive cases are either HHV-6 variant A or B, and whether HHV-6 mRNA as well as a high copy numbers of HHV-6 DNA can be detected in positive samples.

MATERIALS AND METHODS

Subjects

The first patient group was examined between 2006 and 2010 at the Tokyo Medical and Dental University Hospital, Kyoto Prefectural University Hospital, and Shinkawabashi Hospital in Japan. After informed consent was obtained, ocular fluid samples were collected from patients with uveitis (infectious and noninfectious) or endophthalmitis. This group included consecutive patients with uveitis or endophthalmitis ($n = 350$), including a previously HHV-6-positive severe panuveitis case.⁷ Corneal tissues were also collected from patients with ocular surface diseases (e.g., keratitis, $n = 65$). At this time, we excluded ocular tumor diseases (e.g., intraocular lymphoma) from the patient group.

In addition to the patient group, we also analyzed samples from a control group. A total of 100 samples (50 aqueous humor and 50 vitreous fluids) were collected from patients who did not have any type of ocular inflammation (age-related cataract, macular edema, retinal

From the ¹Laboratory for Retinal Regeneration, RIKEN Center for Developmental Biology, Kobe, Japan; Departments of ²Ophthalmology & Visual Science and ³Virology, Medical Research Institute, Tokyo Medical and Dental University Graduate School of Medicine and Dental Sciences, Tokyo, Japan; ⁴Department of Ophthalmology, Kyoto Prefectural University of Medicine, Kyoto, Japan; and ⁵Department of Ophthalmology, Shinkawabashi Hospital, Kanagawa, Japan.

Supported by Comprehensive Research on Disability, Health and Welfare, Health and Labour Sciences Research Grants, Ministry of Health, Labour, and Welfare, Japan.

Submitted for publication April 26, 2012; revised May 29, 2012; accepted June 10, 2012.

Disclosure: S. Sugita, None; N. Shimizu, None; K. Watanabe, None; M. Ogawa, None; K. Maruyama, None; N. Usui, None; M. Mochizuki, None

Corresponding author: Sunao Sugita, Laboratory for Retinal Regeneration, RIKEN Center for Developmental Biology, 2-2-3 Minatojima-minamimachi, Chuo-ku, Kobe 650-0047, Japan; sunaoph@cdb.riken.jp.

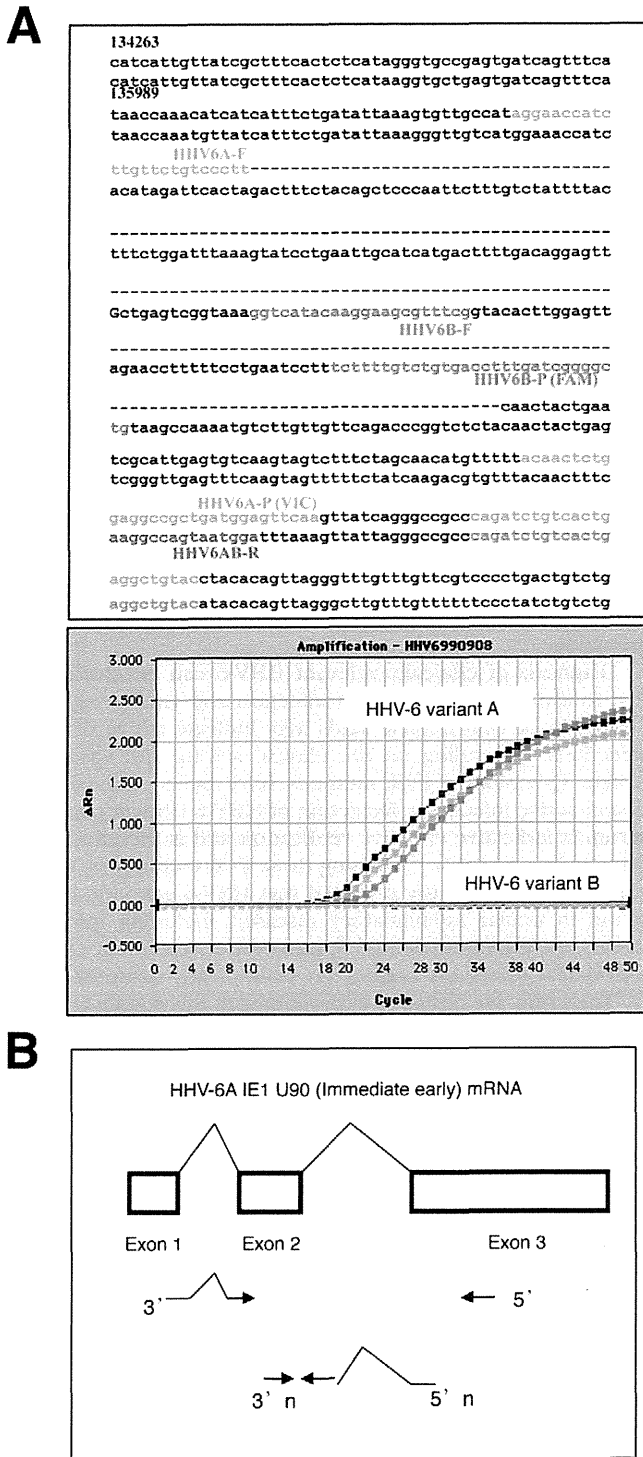


FIGURE 1. Amplification of HHV-6-specific DNA and mRNA. **(A)** TaqMan probes and primers used to amplify HHV-6 DNA (HHV-6A and HHV-6B). HHV-6 subtypes were identified using PCR with variant-specific primers and probes (*lower graph*). **(B)** Nested RT-PCR primers were designed to amplify HHV-6A mRNA.

detachment, idiopathic macular hole, or idiopathic epiretinal membrane).

The research followed the tenets of the Declaration of Helsinki and all study protocols were approved by the Institutional Ethics Committee of Tokyo Medical and Dental University. A clinical trial registration was conducted and information is available at www.umin.ac.jp.

TABLE 1. Clinical Findings in Patients with HHV-6-Associated Ocular Inflammatory Disorders

Case	Age / Sex	Eye	Initial Diagnosis	VA	IOP	Cornea	AC	KPs	VO	Fundus	Bacterial Examination*	Final Diagnosis
1	75 / Male	R	Pan-uveitis	0.02	15	None	Hypopyon	Mutton fat	Grade III	Retinal exudates	Culture (-) / PCR (-)	Ocular toxocariasis
2	64 / Female	L	Corneal endothelitis	0.5	33	Edema	Cell 2+	Mutton fat	None	None	PCR (-)	HSV-1 corneal endothelitis
3	70 / Male	L	Bacterial endophthalmitis	sl	35	None	Hypopyon	Fine	Grade III	Retinal necrosis	Culture (+) / PCR (+)	Endogenous endophthalmitis
4	74 / Female	R	Idiopathic uveitis	0.8	16	None	Cell 1+	None	Grade II	None	PCR (+)	Late postoperative endophthalmitis
5	79 / Female	L	Bacterial endophthalmitis	mm	19	None	Hypopyon	Fine	Grade II	Retinal exudates, hemorrhage	Culture (+) / PCR (+)	Acute postoperative endophthalmitis
6	71 / Female	L	Necrotic retinitis	0.04	12	None	None	None	None	Retinal necrosis, hemorrhage	PCR (-)	Cytomegalovirus retinitis
7	24 / Female	L	Posner-Schlossman synd.	1.2	24	None	Cell 1+	Mutton fat	None	None	PCR (-)	Idiopathic uveitis
8	22 / Male	R	Keratitis	0.7	15	Infiltration	Cell 1-	None	None	None	Culture (-) / PCR (+)	Bacterial keratitis

* Bacterial examination: Results for bacterial culture and/or PCR (bacterial 16S rDNA). AC, anterior chamber; KPs, keratic precipitates; VA, visual acuity by Landolt Chart; VO, vitreous opacity.

TABLE 2. Virological Analysis and Treatment in Patients with HHV-6-Associated Ocular Inflammatory Disorders

Case	Ocular Sample	HHV Genome	Viral Copy No. by Real-Time PCR	HHV-6A or B	Treatment
1	Aqh	HHV-6	HHV-6: 2.4×10^6 copies/mL	HHV-6A	PSL, PPV, VCV, VGV
	VF	HHV-6, EBV	HHV-6: 2.0×10^4 copies/mL, EBV: <50 copies/mL		
2	Aqh	HHV-6, HSV-1	HHV-6: 7.5×10^3 copies/mL, HSV-1: 2.8×10^5 copies/mL	HHV-6B	VGV
3	VF	HHV-6	HHV-6: 5.1×10^6 copies/mL	HHV-6B	PPV, SA, IAI
4	VF	HHV-6	HHV-6: 1.1×10^4 copies/mL	HHV-6B	PPV, VGV
5	VF	HHV-6	HHV-6: 1.1×10^6 copies/mL	HHV-6B	PPV, SA, Betametasone
6	VF	HHV-6, CMV	HHV-6: 4.4×10^4 copies/mL, CMV: 1.6×10^6 copies/mL	HHV-6A	VGV
7	Aqh	HHV-6	HHV-6: 4.0×10^3 copies/mL	HHV-6B	None
8	Cornea	HHV-6	HHV-6: 3.9×10^6 copies/ μ g · DNA	HHV-6B	Antibiotics

Aqh, aqueous humor; IAI, intravitreal antibiotic injection; PPV, pars plana vitrectomy; PSL, prednisolone; SA, systemic antibiotics; VCV, valacyclovir; VF, vitreous fluids; VGV, valganciclovir.

ac.jp/ctr/index/htm with study number of R000002708. The study started in April 2006 and terminated in April 2010.

PCR

DNA was extracted from samples using an E21 virus minikit (Qiagen, Valencia, CA) installed on a robotic workstation for automated purification of nucleic acids (BioRobot E21, Qiagen). HHV genomic DNA in ocular samples was detected using two independent PCR assays: a qualitative multiplex PCR and a quantitative real-time PCR.¹⁶

The multiplex PCR was designed to qualitatively measure genomic DNA of eight human herpes viruses as follows: herpes simplex virus type 1 (HSV-1), type 2 (HSV-2), Varicella-zoster virus (VZV), Epstein-Barr virus (EBV), cytomegalovirus (CMV), and human herpes virus 6 (HHV-6), 7 (HHV-7), and 8 (HHV-8). PCR was performed using a LightCycler (Roche, Rotkreuz, Switzerland). Primers for HHV-6 were as follows: Forward - ACCCGAGAGATGATTTTGC and Reverse - GCAGAAGACAGCAGCGAGAT. Probes were used as follows: 3'^{FITC}-TAAG-TAACCGTTTTCGTCCCA and LcRed705-5'-GGGTCATTATGTTATAGA. These primers and probes do not distinguish between HHV-6A and B. PCR conditions, primers, and probes specific for other HHV have been described previously.¹⁷

Real-time PCR was performed for detection of HHV only, following identification of genomic DNA by multiplex PCR. Real-time PCR was performed using Amplitaq Gold and the Real-Time PCR 7300 system (ABI, Foster City, CA). The sequence of the HHV-6 primers and probes are as follows: Forward - GACAATCACATGCCTGGATAATG and Reverse - TGTAAGCGTGTGTAATGTACTAA. The probe was AG-CAGCTGGCGAAAAGTGTGTGC. The primers and probes of other herpes viruses and the PCR conditions have been described previously.^{16,17} These primers and probes do not distinguish between HHV-6A and B. TaqMan probes and primers used in the HHV-6 DNA amplifications, HHV-6 type A and HHV-6 type B, are shown in Figure 1A. The value of viral copy number in the sample was considered to be significant when more than 50 copies/mL were observed.

RT-PCR

The primers for nested RT-PCR were designed to detect mRNA (HHV-6 A IE1 U90 immediate early) as follows: first PCR Forward - GATGAACGTATGCAAGACTACC and ATGAACATGGATTGTTGCTG and Reverse - CAGCGACTGAGCAGCTA; nested PCR Forward - CCGATCCAATGATGGAAGAA and Reverse - CAGCGACTGAGCAGCTA (Fig. 1B). A one-step RT-PCR was performed on 100 ng of total RNA with 0.5 μ M of each primer and SuperScript III One-Step RT-PCR with platinum Taq (Life Technologies Co., Tokyo, Japan) in a final volume of 50 μ L. Samples were reverse transcribed for 30 minutes at 54°C and amplified for 40 cycles consisting of denaturation for 15 seconds at 94°C, annealing for 30 seconds at 54°C, and polymerization for 20 seconds at 72°C. Following identification of a PCR product of 340 bp, nested PCR was performed on 1 μ L of the first PCR solution using 0.5

μ M of each primer and 200 mM deoxynucleotide triphosphates and 1.25 U of Taq DNA polymerase (Thermo Fisher Scientific, Tokyo, Japan). Monoclonal antibody (anti-taq high: Toyobo Life Science, Tokyo, Japan) was used at 0.25 μ g in a buffer containing 75 mM Tris-HCl (pH = 8.8), 0.01% Tween-20, 20 mM (NH₄)₂SO₄, and 1.5 mM MgCl₂ in a final volume of 50 μ L. Twenty cycles of amplification consisting of denaturation for 15 seconds at 94°C, annealing for 30 seconds at 55°C, and polymerization for 15 seconds at 72°C were performed to give a positive PCR product of 198 bp.

All ocular samples were tested for the presence of β -actin as an internal control. β -Actin mRNA RT-PCR was performed on 100 ng of total RNA with 0.5 μ M each primer and SuperScript III One-Step RT-PCR with platinum Taq in a final volume of 50 μ L (Forward-CTTCCTTCCTGGGCAT and Reverse-TCTTCATTGTGCTGGGT). Samples were reverse transcribed for 30 minutes at 55°C followed by 40 cycles of denaturation for 30 seconds at 94°C, annealing for 30 seconds at 60°C, and polymerization for 1 minute at 72°C on a thermal cycler TP-400 instrument (Takara Bio Inc., Tokyo, Japan). Raji cell lines were used as a positive control, and MOLT-4 cells were used as a negative control. PCR products were analyzed using 2% agarose gel electrophoresis and ethidium bromide staining and the positive product was 215 bp.

RESULTS

Detection of HHV-6 Genomic DNA in Patients with Uveitis, Endophthalmitis, and Ocular Surface Diseases

We first performed multiplex PCR to screen for 8 HHVs after collecting intraocular samples from patients with various ocular inflammatory diseases. PCR results indicated that 7 (2%) of 350 patients with uveitis or endophthalmitis were positive for HHV-6 DNA. In addition, 1 (1.5%) of 65 patients tested positive for HHV-6 in a corneal tissue sample. These HHV-6-positive cases together with clinical findings are summarized in Tables 1 and 2. These eight HHV-6-positive patients were clinically suspected to have HHV-6-associated infectious diseases based on the detection of HHV-6 genome in ocular fluid or corneal tissue samples. HHV-6 DNA was not detected in any of the 100 control samples that were collected from patients without ocular inflammation.

The clinical features observed in HHV-6-positive cases at their initial presentation are summarized in Table 1. Almost all of the patients with uveitis and endophthalmitis had active ocular inflammation, that is, there were anterior chamber cells (except case 6), keratic precipitates (except cases 4 and 6), vitreous opacity (except cases 2 and 7), and fresh retinal exudates/necrosis (except cases 2, 4, and 7). In the single patient with HHV-6⁺ keratitis (case 8 in Table 1), corneal

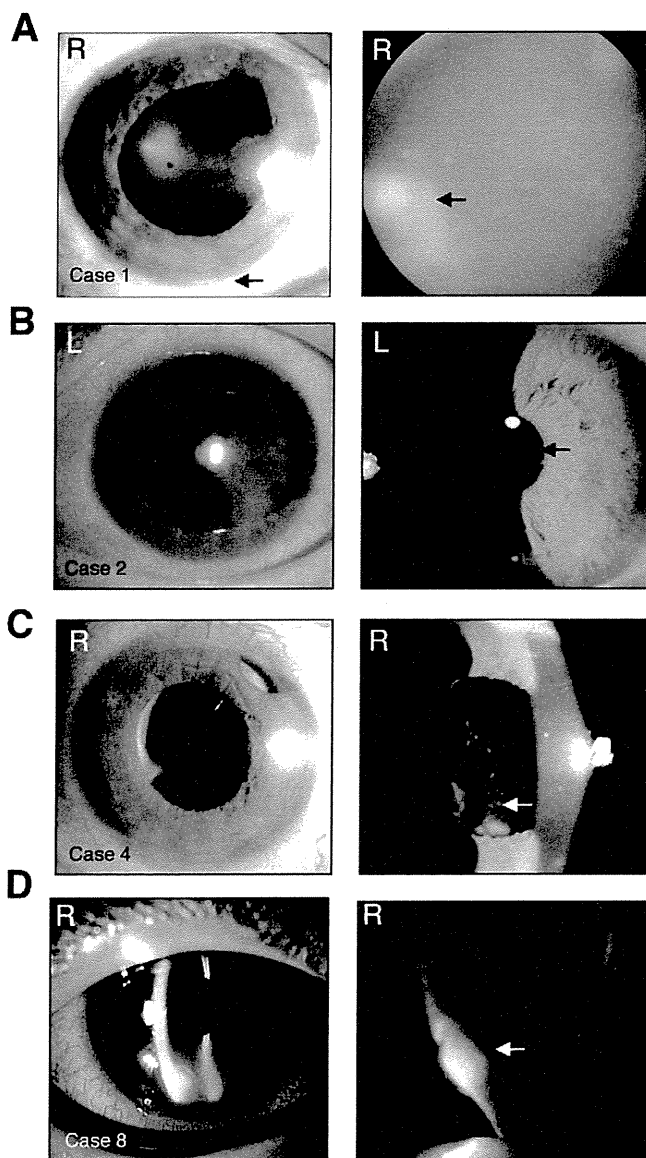


FIGURE 2. Slit-lamp and fundus photographs for HHV-6 infections. (A) Case 1: A case of ocular toxocariasis. Slit-lamp examination of right eye (RE) disclosed ciliary injection, moderate mutton-fat keratic precipitates (KPs), and severe anterior chamber cells with hypopyon (arrow). Funduscopic examination of the RE revealed dense vitreous opacities and yellowish white massive retinal lesions (arrow) in the peripheral fundus. HHV-6 DNA was detected in both aqueous humor and vitreous samples. (B) Case 2: A case of HSV-1-associated corneal endotheliitis. Slit-lamp examination of left eye (LE) disclosed pigmented mutton-fat-like KPs with high intraocular pressure, mild anterior chamber cells, and small-size corneal stromal edema (arrow). HSV-1 and HHV-6 DNA were detected in aqueous humor, but other HHV-DNA, such as VZV and CMV, was not detected. (C) Case 4: A case of late postoperative endophthalmitis. This patient with Vogt-Koyanagi-Harada disease had postcataract surgery 6 months earlier. Slit-lamp examination of RE disclosed ciliary injection and mild anterior chamber cells. White plaque (arrow) on the intraocular lens and mild inflammation were seen, and an aqueous humor sample was obtained. HHV-6 DNA and *Propionibacterium acnes* DNA were detected in the aqueous humor sample. The final diagnosis was *P. acnes*-associated late postoperative endophthalmitis. (D) Case 8: A case of bacterial keratitis (arrow) with ciliary injection. A corneal infiltration with epithelial defect was observed and a high copy number of HHV-6 DNA was detected in corneal tissue samples.

infection, such as corneal epithelial ulcer and ciliary injection, was indicated. Representative findings including slit-lamp or fundus photographs for HHV-6-positive cases are shown in Figure 2. In addition, ocular samples from all patients were subjected to bacterial examinations, including conventional bacterial culture and bacterial broad-range PCR (bacterial 16S rDNA)¹⁸ (Table 1). The final diagnoses were as follows: case 1, ocular toxocariasis; case 2, HSV-1 corneal endotheliitis; case 3, endogenous endophthalmitis; case 4, late postoperative endophthalmitis; case 5, acute postoperative endophthalmitis; case 6, CMV retinitis; case 7, idiopathic uveitis; case 8, bacterial keratitis (Table 1).

We next summarized the virological analysis of ocular samples from these eight HHV-6-positive patients (3 aqueous humor, 5 vitreous fluids, and 1 corneal tissue) in Table 2. Multiplex PCR was used to detect HHV infection (HSV-1, HSV-2, VZV, EBV, CMV, HHV-6, HHV-7, and HHV-8). HHV-6 was found together with EBV (only case 1), HSV-1 (only case 2), or CMV (only case 6). Figure 3 is representative of the results of the multiplex PCR where HHV-6 DNA was detected in aqueous and vitreous fluid from case 1. HHV DNA in nine ocular samples from eight cases was also measured by real-time PCR. These patients had high copy numbers of HHV-6 DNA, with values ranging from 4.0×10^3 to 5.1×10^6 copies/mL (Table 2), suggesting that viral replication may occur in the eye. Following diagnosis, 4 patients received antiviral treatment (i.e., valacyclovir or valganciclovir), which controlled their ocular inflammation (Table 2).

Detection of HHV-6 Variant A or B in Patients with HHV-6-Associated Ocular Inflammatory Disorders

HHV-6 can be classified into two groups: a variant A (HHV-6A) and a variant B (HHV-6B).¹³ Distinguishing between HHV-6 subtypes is mainly accomplished using PCR techniques, including melting curve¹⁹ or variant-specific primers.²⁰ Therefore, we next determined whether the HHV-6-positive cases were HHV-6A or B using real-time PCR. In this study, we designed a probe and primers for use in the HHV-6 DNA amplification. The paired primers and TaqMan probes used for detection of HHV-6A and HHV-6B are shown in Figure 1A. By using several different primers and probes, we were able to detect each of these HHV-6 types separately (Fig. 1A). The PCR results from case 1 showed that intraocular samples included HHV-6A but not HHV-6B DNA (Fig. 4). Final analysis with quantitative PCR indicated that two of the cases were positive for HHV-6A and six cases were positive for HHV-6B (Table 2).

Detection of HHV-6 mRNA in Intraocular Samples

RT-PCR has previously been used on mRNA from peripheral blood mononuclear cells to detect actively replicating virus.²¹ We therefore tested ocular samples for the presence of HHV-6 mRNA. Various samples, such as aqueous humor, vitreous fluid, retinal membrane tissues, and collected vitreous cells from an HHV-6A-positive case (case 1), were available for the RT-PCR assay. We designed primers to amplify mRNA using a nested RT-PCR (HHV-6 A IE1 U90, Fig. 1B). As revealed in Figure 5, HHV-6A mRNA was clearly detected in vitreous cell samples, but other ocular samples from the same patient were all negative.

DISCUSSION

In this study, we demonstrate that seven patients with uveitis or endophthalmitis were positive for HHV-6 DNA. In addition, one patient with infectious keratitis was also found to be HHV-6-positive. These patients had high copy numbers of HHV-6

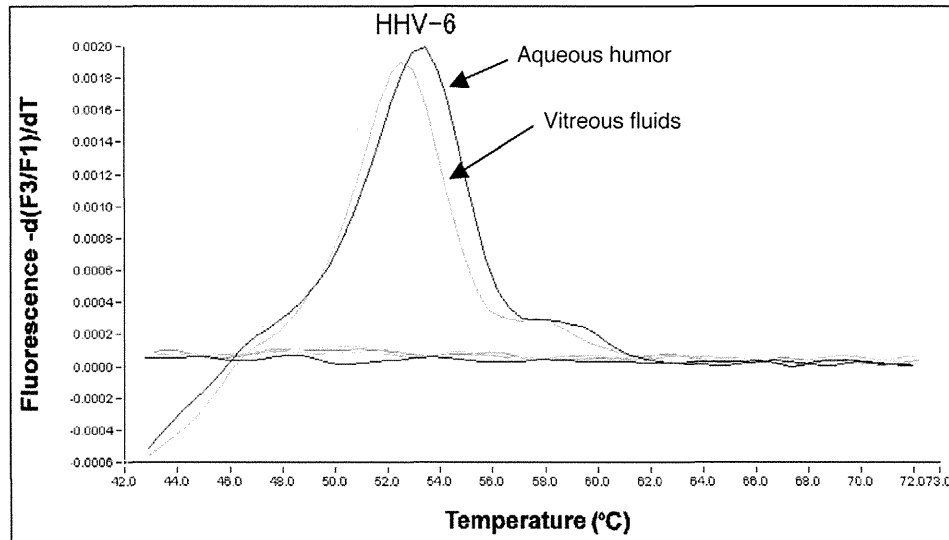


FIGURE 3. Results for multiplex PCR in a patient with HHV-6-positive uveitis. A significant positive curve was seen at 52°C, indicating detection of HHV-6 genomic DNA in the ocular fluids (case 1). DNA from other herpes viruses, such as HSV1, HSV2, VZV, EBV, CMV, HHV7, and HHV8, was not detected in this sample.

DNA, and two cases were found to be HHV-6 type A and six cases were type B. In addition, HHV-6 mRNA was detected in intraocular samples from HHV-6-positive patients, suggesting that viral replication or reactivation may occur in the eye.

Recently, Cohen et al.⁵ reported that HHV-6A DNA could be detected by PCR in vitreous fluid from a patient with CMV-associated retinitis when vitreous fluids were assayed from 101 patients with ocular inflammation for HHV-6A, HHV-6B, and HHV-7. HHV-6B DNA was also detected in vitreous fluid from a patient with idiopathic uveitis in the absence of CMV DNA. This study suggests that HHV-6A and HHV-6B DNA are detectable in approximately 1% of vitreous samples from patients with ocular inflammation. In our study, we show that HHV-6 DNA was detectable in 2% of ocular samples from patients with intraocular inflammation following screening for HHV-1 to -8 infection using multiplex PCR.

In a previous study,¹⁶ we found that intraocular HHV DNA was detectable in a wide range of herpes virus-associated uveitis cases when analysis was performed using multiplex PCR. PCR is a valuable tool for the diagnosis of herpetic uveitis and it is now possible to exclude nonherpetic uveitis patients using this method. Moreover, de Boer et al.⁸ previously found that in patients with herpetic anterior uveitis, PCR was more frequently positive than the Goldmann-Witmer coefficient. HHV-6 has been implicated in ocular inflammation, most remarkably when the posterior segment of the eye was affected.^{6,7,10-12} On the other hand, the role of HHV-6 as a cause of anterior uveitis is inconclusive and further studies are required. As revealed in this study, we found three cases of anterior inflammatory diseases including keratitis and five cases of pan- or posterior inflammatory diseases in the eye.

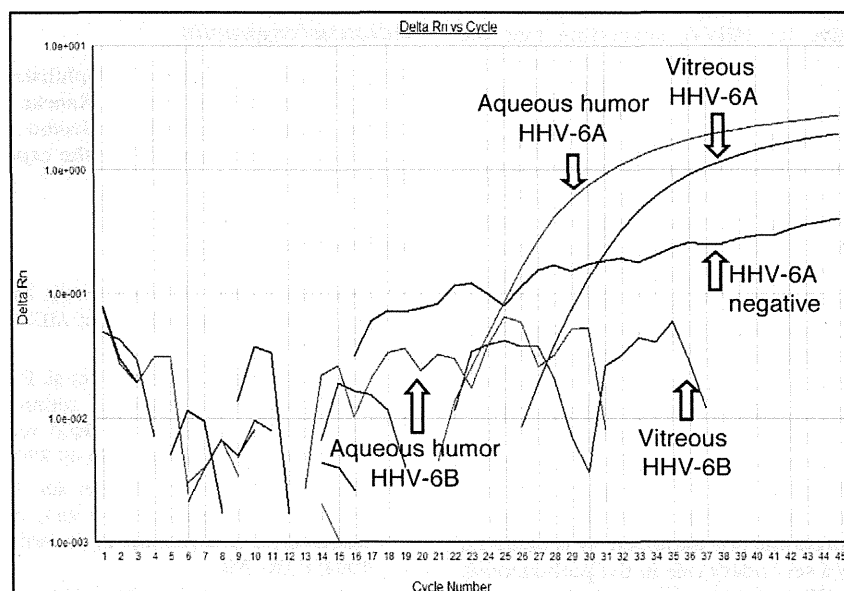


FIGURE 4. Detection of HHV-6 DNA by quantitative real-time PCR. The real-time PCR results for the samples from case 1 showed that intraocular samples, such as aqueous humor and vitreous fluids, contained a high copy number of HHV-6A DNA, but not HHV-6B DNA.

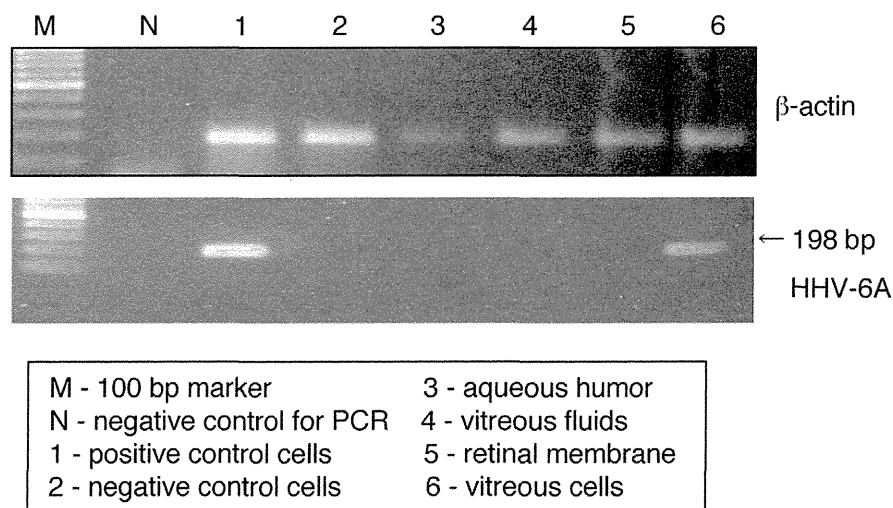


FIGURE 5. Detection of HHV-6 mRNA in intraocular samples. HHV-6A mRNA was detected in samples from vitreous cells, but other ocular samples, such as aqueous humor, vitreous fluids, and retinal membrane tissues were all negative (*lower image*). All samples, including control RNA, were positive for β -actin (*upper image*).

The detection of HHV-6 in the eye might not be clinically relevant. HHV-6 can latently reside in cells of the lymphoid and myeloid lineage and it may have entered the inflamed eye via immune cells, similar to EBV and human immunodeficiency virus.^{3,22,23} Thus, HHV-6 DNA has been detected in circulating T cells, monocytes, and leukocytes and may simply have been carried into the eyes in the inflammatory cells as a result of destruction of the blood-retina barrier. Our data indicate that most HHV-6 DNA in intraocular fluids of inflamed eyes might be a consequence of the release of HHV-6 DNA from resident ocular cells caused by intraocular inflammation. A high copy number of HHV-6 DNA was detected in patients with severe ocular inflammation, pan- or posterior uveitis, or endophthalmitis (Tables 1 and 2). This is supported by the findings of Arao et al.,²⁴ who showed that HHV-6 can infect human retinal pigment epithelial cells.

We detected HHV-6 in only one patient with an ocular surface inflammatory disorder. The patient was a young healthy donor suffering from atopic dermatitis. Okuno et al.⁹ recently reported that 14 of 22 patients with corneal inflammation were positive for HHV-6, suggesting that the association of HHV-6 with disease was more frequent than with other herpes viruses, such as HSV-1. Thus, HHV-6 may be another sole causative agent of corneal inflammation.

HHV-6 reactivation frequently accompanies CMV reactivation,²⁵ and the presence of HHV-6A DNA in the eye may simply reflect the immunocompromised state of the patient. Case 6 in this study was a patient with CMV retinitis who was also found to be HHV-6A DNA-positive; however, with the exception of this patient, our HHV-6 PCR-positive patients were neither young nor immunosuppressed. We previously used multiplex PCR to search for HHV-6 in ocular fluids from 100 patients with uveitis and detected HHV-6A DNA in one patient with severe unilateral uveitis (case 1).⁷ This patient's ocular fluid also contained antibodies to *Toxocara canis* larvae and we finally diagnosed ocular toxocariasis and HHV-6-related pan-uveitis.⁷ In this study, 7 patients were found to have other infectious agents, including bacteria, other herpes viruses (HSV-1), and parasites (*Toxocara*); however, it is unclear whether HHV-6 was the predominant pathogen. It is assumed that HHV-6 infections play a secondary role in the pathogenesis of ocular inflammation. Therefore, we tested intraocular samples for the presence of HHV-6 mRNA. Additional tests for HHV-6 RNA or protein in ocular tissues would have been

more definitive and provided evidence of HHV-6 replication. We found HHV-6A mRNA and a high copy number of HHV-6 DNA in the same sample from a patient with ocular toxocariasis (case 1). As far as we know, this is the first report of detection of both HHV-6 DNA and mRNA in an ocular sample. The RT-PCR assay can reliably differentiate between latent and actively replicating HHV-6 and its use should allow an insight into the pathogenesis of this ubiquitous virus as previously reported.²¹

In conclusion, ocular samples collected from patients with infectious ocular disorders can contain a high copy number of HHV-6 DNA. The HHV-6-positive case was found to have HHV-6 DNA and mRNA in the inflamed eye. We are currently conducting experiments to determine whether HHV-6 type A and type B can infect ocular cells, such as retinal pigment epithelium, *in vitro*. Infected ocular cells can produce inflammatory cytokines and chemokines that differ from those in normal uninfected cells.

Acknowledgments

Kenji Nagata (Department of Ophthalmology, Kyoto Prefectural University of Medicine) and Yu Kaneko (Department of Ophthalmology, Yamagata University) collected and sent the samples used in this study. We are grateful for the expert technical assistance of Shizu Inoue.

References

1. Qavi HB, Green MT, Pearson G, Ablashi D. Possible role of HHV-6 in the development of AIDS retinitis. *In Vivo*. 1994;8:527-532.
2. Fillet AM, Reux I, Joberty C, et al. Detection of human herpes virus 6 in AIDS-associated retinitis by means of *in situ* hybridization, polymerase chain reaction and immunohistochemistry. *J Med Virol*. 1996;49:289-295.
3. Mitchell SM, Fox JD, Tedder RS, Gazzard BG, Lightman S. Vitreous fluid sampling and viral genome detection for the diagnosis of viral retinitis in patients with AIDS. *J Med Virol*. 1994;4:336-340.
4. de Groot-Mijnes JD, de Visser L, Zuurveen S, et al. Identification of new pathogens in the intraocular fluid of patients with uveitis. *Am J Ophthalmol*. 2010;150:628-636.

5. Cohen JI, Fahle G, Kemp MA, Apakupakul K, Margolis TP. Human herpesvirus 6-A, 6-B, and 7 in vitreous fluid samples. *J Med Virol.* 2010;82:996-999.
6. Maslin J, Bigaillon C, Froussard F, Enouf V, Nicand E. Acute bilateral uveitis associated with an active human herpesvirus-6 infection. *J Infect.* 2007;54:237-240.
7. Sugita S, Shimizu N, Kawaguchi T, Akao N, Morio T, Mochizuki M. Identification of human herpesvirus 6 in a patient with severe unilateral panuveitis. *Arch Ophthalmol.* 2007;125:1426-1427.
8. de Boer JH, Verhagen C, Bruinenberg M, et al. Serologic and polymerase chain reaction analysis of intraocular fluids in the diagnosis of infectious uveitis. *Am J Ophthalmol.* 1996;121:650-658.
9. Okuno T, Hooper LC, Ursea R, et al. Role of human herpes virus 6 in corneal inflammation alone or with human herpesviruses. *Cornea.* 2011;30:204-207.
10. Mechai F, Boutolleau D, Manceron V, et al. Human herpesvirus 6-associated retrobulbar optic neuritis in an HIV-infected patient: response to anti-herpesvirus therapy and long-term outcome. *J Med Virol.* 2007;79:931-934.
11. Moschetti D, Franceschini R, Vaccaro NM, et al. Human herpesvirus-6B active infection associated with relapsing bilateral anterior optic neuritis. *J Clin Virol.* 2006;37:244-247.
12. Oberacher-Velten IM, Jonas JB, Jünemann A, Schmidt B. Bilateral optic neuropathy and unilateral tonic pupil associated with acute human herpesvirus 6 infection: a case report. *Graefes Arch Clin Exp Ophthalmol.* 2005;43:175-177.
13. Schirmer EC, Wyatt LS, Yamanishi K, Rodriguez WJ, Frenkel N. Differentiation between two distinct classes of viruses now classified as human herpesvirus 6. *Proc Natl Acad Sci U S A.* 1991;88:5922-5926.
14. Huang LM, Kuo PF, Lee CY, Chen JY, Liu MY, Yang CS. Detection of human herpesvirus-6 DNA by polymerase chain reaction in serum or plasma. *J Med Virol.* 1992;38:7-10.
15. Suga S, Yazaki T, Kajita Y, Ozaki T, Asano Y. Detection of human herpesvirus 6 DNAs in samples from several body sites of patients with exanthem subitum and their mothers by polymerase chain reaction assay. *J Med Virol.* 1995;46:52-55.
16. Sugita S, Shimizu N, Watanabe K, et al. Use of multiplex PCR and real-time PCR to detect human herpes virus genome in ocular fluids of patients with uveitis. *Br J Ophthalmol.* 2008;92:928-932.
17. Sugita S, Iwanaga Y, Kawaguchi T, et al. Detection of herpesvirus genome by multiplex polymerase chain reaction (PCR) and real-time PCR in ocular fluids of patients with acute retinal necrosis. *Nippon Ganka Gakkai Zasshi.* 2008;112:30-38.
18. Sugita S, Shimizu N, Watanabe K, et al. Diagnosis of bacterial endophthalmitis by broad-range quantitative polymerase chain reaction. *Br J Ophthalmol.* 2011;95:345-349.
19. Razonable RR, Fanning C, Brown RA, et al. Selective reactivation of human herpesvirus 6 variant A occurs in critically ill immunocompetent hosts. *J Infect Dis.* 2002;185:110-113.
20. Boutolleau D, Duros C, Bonnafous P, et al. Identification of human herpesvirus 6 variants A and B by primer-specific real-time PCR may help to revisit their respective role in pathology. *J Clin Virol.* 2006;35:257-263.
21. Norton RA, Caserta MT, Hall CB, Schnabel K, Hocknell P, Dewhurst S. Detection of human herpesvirus 6 by reverse transcription-PCR. *J Clin Microbiol.* 1999;37:3672-3675.
22. Rothova A, de Boer JH, Ten Dam-van NH, et al. Usefulness of aqueous humor analysis for the diagnosis of posterior uveitis. *Ophthalmology.* 2008;115:306-311.
23. Ongkosuwito JV, Van der Lelij A, Bruinenberg M, et al. Increased presence of Epstein-Barr virus DNA in ocular fluid samples from HIV negative immunocompromised patients with uveitis. *Br J Ophthalmol.* 1998;82:245-251.
24. Arai Y, Souchi S, Sato Y, et al. Infection of a human retinal pigment epithelial cell line with human herpesvirus 6 variant A. *J Med Virol.* 1997;53:105-110.
25. Humar A, Malkan G, Moussa G, Greig P, Levy G, Mazzulli T. Human herpesvirus-6 is associated with cytomegalovirus reactivation in liver transplant recipients. *J Infect Dis.* 2000;181:1450-1453.

Novel diagnosis of fungal endophthalmitis by broad-range real-time PCR detection of fungal 28S ribosomal DNA

Manabu Ogawa · Sunao Sugita · Ken Watanabe ·
Norio Shimizu · Manabu Mochizuki

Received: 16 January 2012 / Revised: 21 March 2012 / Accepted: 22 March 2012
© Springer-Verlag 2012

Abstract

Aim To detect the fungal genome in the ocular fluids of patients with fungal endophthalmitis by using a novel broad-range polymerase chain reaction (PCR) system.

Methods After informed consent was obtained, ocular fluid samples (aqueous humor or vitreous fluids) were collected from 497 patients (76 patients with infectious endophthalmitis including clinically suspected bacterial and fungal endophthalmitis and 421 patients with infectious or non-infectious uveitis). Forty ocular samples from non-infectious patients without ocular inflammation were collected as controls. Fungal ribosomal DNA (28 S rDNA) was measured by a quantitative real-time PCR assay.

Results Fungal 28 S rDNA of the major fungal species, such as *Candida*, *Aspergillus*, and *Cryptococcus*, were detected by novel broad-range real-time PCR examination ($>10^1$ copies/ml). Fungal 28 S rDNA was detected in the ocular fluids of 11 patients with endophthalmitis or uveitis (11/497, 2.2%). All 11 positive samples were detected in the infectious endophthalmitis patients (11/76, 14.5%). These PCR-positive ocular fluids had high copy numbers of fungal 28 S rDNA (range, 1.7×10^3 to 7.9×10^6 copies/ml), which

indicated the presence of fungal infection. Of the 11 patients who were PCR positive, further examinations led to a diagnosis of fungal endophthalmitis in ten patients. The fungal 28 S rDNA was detected in one non-infectious case (a false-positive case). In addition, there were two PCR false-negative cases that were clinically suspected of having fungal endophthalmitis.

Conclusions This novel quantitative broad-range PCR of fungal 28 S rDNA is a useful tool for diagnosing endophthalmitis related to fungal infections.

Keywords Polymerase chain reaction · Fungi · Ocular fluids · Endophthalmitis

Introduction

Fungal endophthalmitis can be caused by endogenous infections. These infections occur in patients who have systemic disorders (e.g., diabetes or malignancy), patients who use systemic drugs (e.g., broad-spectrum antibiotics, chemotherapeutic agents, or steroids), and patients who have intravascular catheters. In addition, fungal endophthalmitis can be caused by exogenous infections that arise from trauma or intraocular surgery. The clinical findings in some ocular infectious diseases caused by fungal species are quite diverse, with the exception of *Candida* infection. *Candida* infection in the eye is always characterized as endogenous endophthalmitis with fungal ball vitreous opacities. Moreover, fungal infections have been widely associated with various ocular disorders including endophthalmitis. Because of this diversity, it is often difficult to diagnose ocular fungal infections. Polymerase chain reaction (PCR) has been used to provide evidence of fungal involvement in suspected cases of intraocular infections. Previous studies have used PCR to demonstrate the presence of

M. Ogawa · S. Sugita (✉) · M. Mochizuki
Department of Ophthalmology & Visual Science,
Tokyo Medical and Dental University Graduate
School of Medicine,
1-5-45 Yushima, Bunkyo-ku,
Tokyo 113-8519, Japan
e-mail: sunaoph@tmd.ac.jp

K. Watanabe · N. Shimizu
Department of Virology, Division of Medical Science,
Tokyo Medical and Dental University,
Graduate School of Medical and Dental Sciences,
Tokyo, Japan

fungal DNA in the ocular fluids of patients with infectious endophthalmitis [1–3].

PCR-based methods make it possible to establish a diagnosis in less time than is required by standard cultures [4–6]. Moreover, studies have found that fungal cultures are negative in half of PCR-positive cases [1–3, 7]. The sensitivity of conventional culture techniques is not high, and these cultures take a long time due to their slow growth. Thus, the use of broad-range real-time PCR to analyze ocular samples may be a better way to obtain a rapid diagnosis in patients with unknown intraocular infectious diseases.

For the diagnosis of infectious endophthalmitis, broad-range real-time PCR for fungi is now available [1–3, 7]. To detect many types of fungal DNA, primers and probes for conserved regions in fungal sequences are used. We previously designed pan-fungal primers and probes that were complementary to the 18 S rRNA sequences present in the *Candida* and *Aspergillus* species, and we reported the efficacy of the technique for diagnosis [7]. This PCR technique detected all species of *Candida* and *Aspergillus* DNA. Although there were many advantages to using this PCR technique to diagnose fungal infection, there was one disadvantage. Although the fungal 18 S broad-range PCR detected *Candida* and *Aspergillus* DNA, it cannot detect other types of fungal DNA. Recently, a novel broad-range real-time PCR technique was developed for the rapid detection of human pathogenic fungi [8]. The assay targeted a part of the 28 S large subunit rRNA genes (28 S rDNA). Therefore, we prepared a new assay that targets a part of the 28 S rDNA found in species such as *Candida*, *Aspergillus*, *Cryptococcus*, *Trichophyton*, *Mucor*, *Penicillium*, and *Pichia*.

In the present study, we attempted to develop a novel fungal PCR examination that uses 28 S rDNA primers and the corresponding probes for the diagnosis of endophthalmitis related to fungal infection.

Materials and methods

Subjects

Based upon medical history and clinical observations, 497 patients (260 men and 237 women) were consecutively enrolled in a prospective study that was conducted at the Tokyo Medical and Dental University Hospital. The patient group consisted of patients with infectious endophthalmitis including clinically suspected bacterial and fungal endophthalmitis ($n=76$) and patients with infectious or non-infectious uveitis ($n=421$). The average patient age (\pm SD) was 60 (\pm 16) years. After obtaining informed consent,

samples of aqueous humor and vitreous fluids were collected from all patients.

In addition to the patient group, we also analyzed samples from a control group in which no patients had any type of ocular inflammation. The control patients were enrolled in this prospective study in 2009. Forty samples (20 aqueous humor samples and 20 vitreous fluid samples) were collected from the 40 control patients. The control group consisted of patients who had age-related cataract ($n=20$), macular edema ($n=14$), retinal detachment ($n=4$), idiopathic macular hole ($n=1$), and idiopathic epiretinal membrane ($n=1$).

For aseptic ocular sampling, the following procedures were performed in all subjects, as described in our previous reports [7, 9]. A 0.1-ml aliquot of aqueous humor was collected aseptically in a syringe with a 30-G needle. Half of the sample was then transferred into a pre-sterilized microfuge tube and used for PCR. In patients who were undergoing vitreous surgery, uncontaminated non-diluted vitreous fluid samples (0.5–1.0 ml) were collected during the diagnostic pars plana vitrectomy [7, 9]. Topical antibiotics were used in almost all patients before collecting samples, but oral antibiotics were not used.

The research followed the tenets of the Declaration of Helsinki, and all study protocols were approved by the Institutional Ethics Committee of Tokyo Medical and Dental University. The clinical trial was registered, and the information is available at www.umin.ac.jp/ctr/index/htm with study number R000002708. The study was started in July 2009 and was terminated in February 2011.

Quantitative polymerase chain reaction

DNA was extracted from the samples using a DNA Mini Kit (Qiagen, Valencia, CA, USA) installed on a Robotic workstation that was set for automated purification of nucleic acids (BioRobot EZ1 Advanced, Qiagen). The real-time PCR was performed by using an Amplitaq Gold and Light Cycler 480 II (Roche, Basel, Switzerland). Primers and probes of fungal 28 S rDNA are described elsewhere [8]. The sense primer was 5'-gcatatcaataagcggaggaaaag-3', and the antisense primer was 5'-ttagcttttagatgRaRttaccacc-3'. The probe (Dual-Labeled probe, Integrated DNA Technologies, Coralville, IA, USA) was 5'-FAM-cggcgagtgaagcgg-SaaRagctc-iowaBK-3'. Products were subjected to 50 cycles of PCR amplification, with cycling conditions set at 95 °C for 10 min, followed by 50 cycles at 95 °C for 0 s and 60 °C for 20 s. For PCR assay sensitivity, PCR fragments were amplified from the DNA of *C. albicans* (strain: ATCC 60193), *A. flavus* (strain: ATCC 22546), and *C. neoformans* (strain: ATCC 14116). The PCR results were obtained within 3 h after sample collection.

Amplification of the human β -globulin gene served as an internal positive extraction and amplification control. Fungal copy number values of more than 100 copies/ml in the sample were considered to be significant.

Results

Sensitivity of broad-range real-time PCR assay for fungal 28 S rDNA

To confirm the broad-range real-time PCR assay sensitivity, PCR fragments were amplified from the DNA of *Candida*, *Aspergillus*, and *Cryptococcus* species. The detection limit and standard range of the TaqMan real-time PCR were determined by using serial tenfold dilutions of linearized plasmid. The PCR results for the prepared samples showed that *C. albicans* DNA was detected at concentrations between 10^2 and 10^5 copies/ml (Fig. 1A). In addition, *Aspergillus* (Fig. 1B) and *Cryptococcus* DNA (Fig. 1C) were also detected at concentrations between 10^2 and 10^5 copies/ml. The best sensitivity for detecting *Candida*, *Aspergillus*, or *Cryptococcus* DNA was at a concentration of 10^1 copies/ml. No DNA was detected in the negative control (nuclease-free water).

Detection of fungal 28 S rDNA in suspected fungal endophthalmitis patients

The PCR results indicated that fungal 28 S rDNA was positive in 11 samples of ocular fluid from the endophthalmitis or uveitis patients (11/497, 2.2%). All 11 positive samples were detected in the infectious endophthalmitis patients (11/76, 14.5%). A representative PCR result in a case of endogenous endophthalmitis related to *Aspergillus* infection is shown in Fig. 2.

The PCR-positive patients had high copy numbers of fungal 28 S rDNA ranging from 1.7×10^3 to 7.9×10^6 copies/ml, which indicated the presence of fungal infection. Further examinations revealed that 10 of the 11 PCR-positive patients had fungal endophthalmitis; seven patients were diagnosed with endogenous endophthalmitis (3 *Candida*, 1 *Aspergillus*, 1 *Cryptococcus*, and 2 unknown), and three patients were diagnosed with late postoperative endophthalmitis (2 *Candida* and 1 unknown) (Table 1). Fungal 28 S rDNA was detected in only one non-infectious case (case 455 in Table 1). This PCR false-positive case had primary intraocular lymphoma that was diagnosed by monoclonal detection of B-cell IgH rearrangement by PCR, high amounts of IL-10 by ELISA, and detection of typical lymphoma cells (Class V) in the vitreous sample. Thus, fungal 28 S rDNA was detected in ocular

samples from 10 patients with fungal endophthalmitis and one patient with non-infectious primary intraocular lymphoma.

However, two of the PCR-negative patients were clinically suspected to have fungal endophthalmitis (cases 24 and 461 in Table 1). PCR did not detect the fungal genome in the aqueous humor of these patients (<100 copies). *C. albicans* was detected in blood samples from case 461. Case 24 was a patient with endogenous endophthalmitis, and his blood tests were positive for β -D-glucan. Systemic antimycotic and topical antimycotic therapies were effective in the treatment of these two patients with false-negative results.

In conventional fungal cultures of ocular fluids, six (60%) of the 10 PCR-positive samples from fungal endophthalmitis patients were positive, and four samples were negative (Table 1). In addition, patients with fungemia (cases 24, 179, 231, 326, 359, 461, and 490) had already begun therapy with antimycotic agents before PCR examinations (Table 2). Among these seven patients, six patients received intravenous hyperalimentation. On the other hand, patients without clinically apparent fungemia (cases 30, 77, 161, and 355) initiated antimycotic drug therapy after receiving positive PCR results (Table 2).

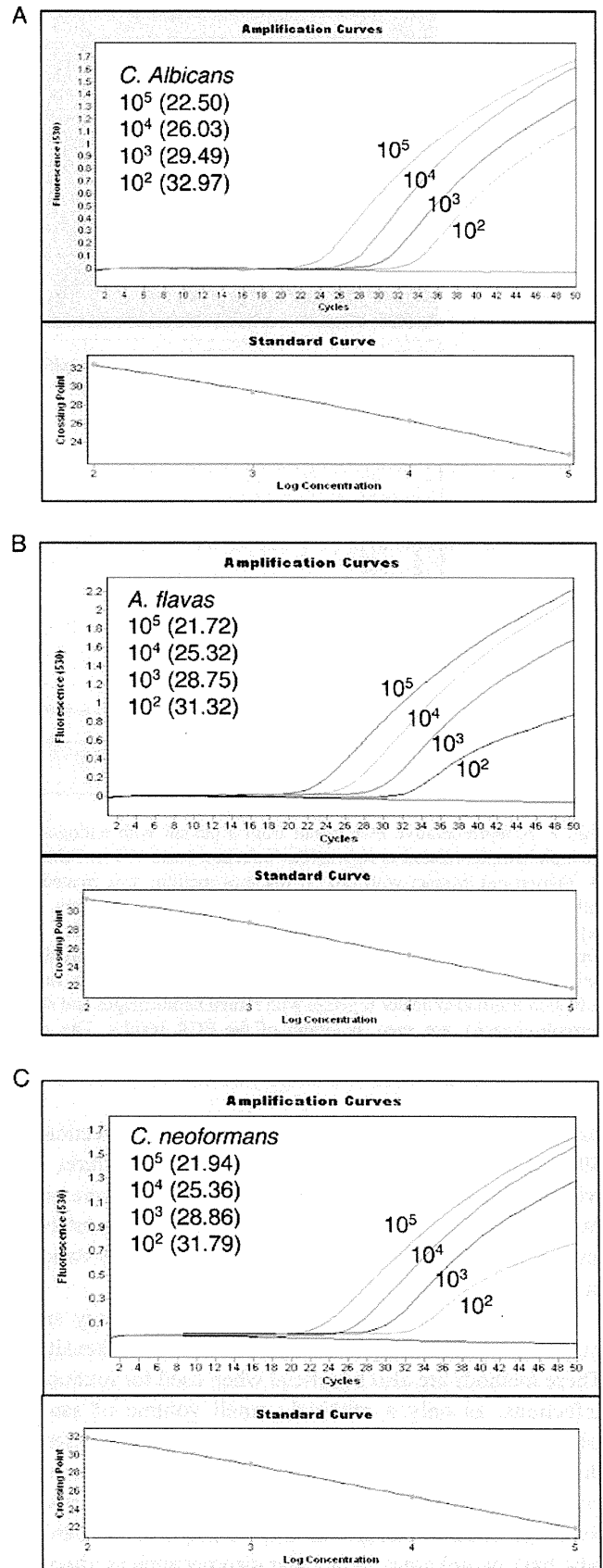
The diagnostic parameters of sensitivity, specificity, positive predictive value, and negative predictive value of the PCR examinations for the diagnosis of fungal endophthalmitis were calculated to be 0.833, 0.998, 0.909, and 0.996, respectively.

Discussion

The broad-range real-time PCR assay amplified fungal 28 S rDNA in the ocular fluids of patients with clinically suspected fungal endophthalmitis. The 28 S rDNA of major fungal species for endophthalmitis, such as *Candida*, *Aspergillus*, and *Cryptococcus*, were detected by a novel broad-range real-time PCR examination ($>10^1$ copies/ml). Our fungal endophthalmitis patients were all immunocompetent, but almost all patients were older than 60 years of age, with the exception of two patients (cases 268 and 490). The PCR examination was negative for fungal DNA in cases of ocular inflammation caused by bacterial endophthalmitis or uveitis. In addition, fungal DNA was not detected in any of the 40 control patients without ocular inflammation.

Broad-range PCR for the 28 S rDNA sequence proved to be a reliable tool for the diagnosis of fungal endophthalmitis. Moreover, real-time quantitative PCR can be used to determine whether or not the fungus is related to the endophthalmitis. By using this PCR system, we were able to rapidly diagnose various types of fungal endophthalmitis in a few

Fig. 1 PCR assay sensitivity. To examine the sensitivity of the broad-range real-time PCR for fungal 28 S rDNA, PCR fragments were amplified from DNA of *Candida* (*C. albicans*, a), *Aspergillus* (*A. flavus*, b), and *Cryptococcus* (*C. neoformans*, c) species. The number in the parenthesis indicates the cycle threshold (Ct) value in quantitative PCR



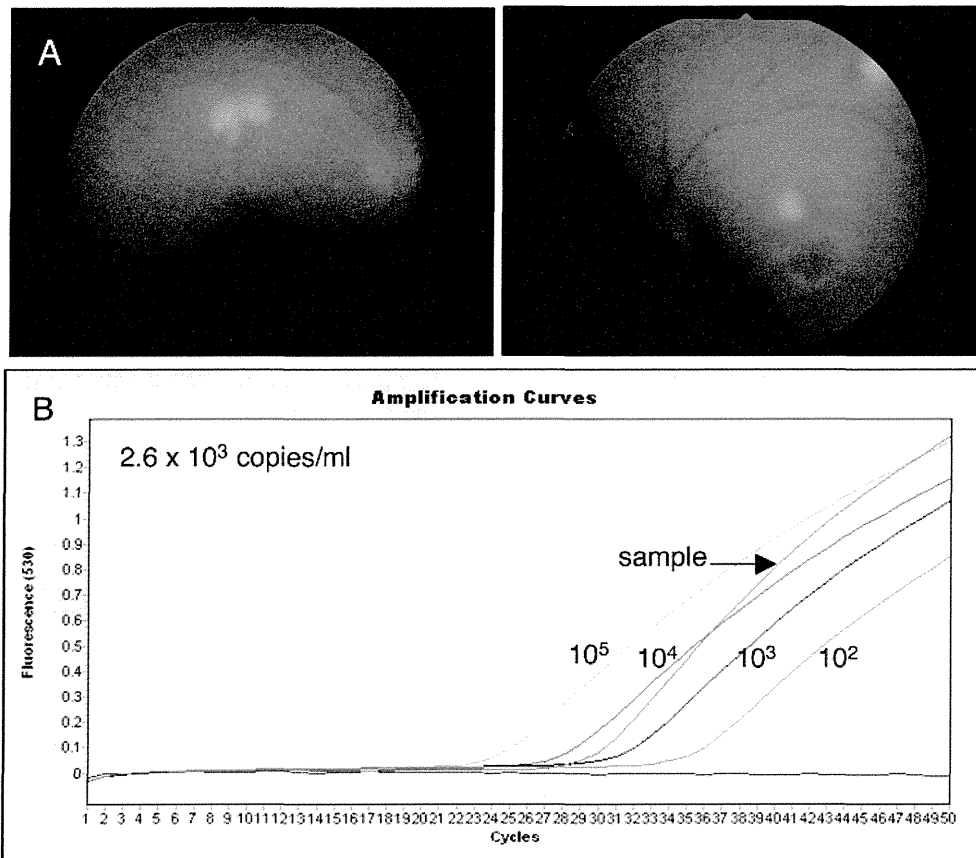


Fig. 2 A representative PCR result from a patient with endogenous endophthalmitis related to *Aspergillus* infection (case 179 in Table 1). A 74-year-old woman with type II diabetes mellitus was treated for splenic cancer. After surgery, she used intravascular catheters. She reported blurred vision and decreased visual acuity in her left eye. Ophthalmologic examination revealed characteristics of infectious endophthalmitis. **a** Fundus photographs of both eyes with a fungal infection. Retinal exudates together with retinal hemorrhages and slight vitreous opacity are seen. **b** Graph of the PCR results. The copy number of fungal genomic DNA in the sample was calculated. Real-

time PCR for the fungal 28 S rDNA was performed with the ocular sample and the control DNA (10^5 , 10^4 , 10^3 , and 10^2 copies/ml). We established the standard curve based on the results from the control DNA. Based on this standard curve, the sample Ct value was used to determine the DNA concentration of the sample. Final copy numbers of genomic DNA in the sample (copies/ml) were calculated based on the original sample volume and the final dilution volume. High copy numbers of fungal 28 S rDNA (2.6×10^3 copies/ml) were detected by real-time PCR

patients exhibiting clinical evidence of a fungal infection. In 40% of the PCR-positive patients, the fungal cultures that were performed on the same ocular fluid sample were negative. Thus, PCR-based methods make it possible to establish an etiologic diagnosis in less time than is required by standard cultures.

In addition, since these methods can detect very small numbers of DNA copies, they are extremely sensitive. These methods are also beneficial when used for intraocular infections, as only a relatively small volume of sample needs to be obtained at any one time. Since it is essential that treatments be started early in cases of infectious endophthalmitis, this broad-range real-time PCR system for ocular samples can provide a rapid diagnosis for patients who have an unknown intraocular disorder such as idiopathic uveitis or endophthalmitis. Additionally, when minimal amounts of ocular samples are available, it is difficult to

perform a culture test to detect fungi [4–6]. Therefore, the use of PCR to detect the fungal genome in ocular fluids is advantageous.

We previously developed a novel PCR assay to detect fungal infection by amplifying fungal 18 S rRNA genes [7]. The broad-range real-time PCR detected a few *Candida* species (*C. albicans*, *C. parapsilosis*, *C. tropicalis*, *C. guilliermondii*, *C. glabrata*, and *C. krusei*), along with *Aspergillus* species (*A. fumigatus*, *A. flavus*, *A. nidulans*, *A. niger*, and *A. terreus*). By using several different primers and probes, we were able to separately detect each of these fungal species. *Candida* or *Aspergillus* DNA was detected in seven of 54 ocular samples (13%) from patients with unknown uveitis or endophthalmitis. These PCR-positive samples showed significantly high copy numbers of *Candida* or *Aspergillus* DNA. On the other hand, fungal DNA was not detected in the other 46 samples collected from these

Table 1 Detection of fungal 28 S rDNA in endophthalmitis and uveitis patients

Case no.	Age/ gender	Diagnosis	Sample	DNA (ng/ml)	Real-time PCR (copies/ml)	Cultures with ocular fluids	Fungal blood test ^a
24	76/M	Endogenous endophthalmitis	AH	26.1	<10 ²	Negative	BDG - 30.2
30	67/F	Late postoperative endophthalmitis	AH	21.4	2.0 × 10 ⁴	<i>Candida albicans</i>	BDG - negative
77	85/M	Endogenous endophthalmitis	VF	41.3	7.6 × 10 ³	<i>Candida</i> spp.	nt
161	75/M	Endogenous endophthalmitis	VF	57.8	2.8 × 10 ⁵	<i>Candida albicans</i>	nt
179	74/F	Endogenous endophthalmitis	AH	29.1	2.6 × 10 ³	Negative	<i>Aspergillus</i> antigen - 36.8
231	64/M	Endogenous endophthalmitis	VF	105	1.7 × 10 ³	Negative	BDG - 11.9
268	40/M	Endogenous endophthalmitis	VF	30.2	2.2 × 10 ⁵	<i>Cryptococcus neoformans</i>	BDG - negative
326	86/F	Endogenous endophthalmitis	VF	85.7	1.5 × 10 ⁵	Negative	BDG - 51.7
355	81/M	Late postoperative endophthalmitis	AH	62.7	7.9 × 10 ⁶	nt	nt
359	69/M	Late postoperative endophthalmitis	VF	20	5.1 × 10 ⁴	<i>Candida</i> spp.	BDG - 36.8
455	67/M	Primary intraocular lymphoma	VF	41.4	5.0 × 10 ⁴	nt	nt
461	63/M	Endogenous endophthalmitis	AH	35.7	<10 ²	Negative	BDG - 24.6; <i>C. acbicans</i>
490	49/M	Endogenous endophthalmitis	AH	43	6.6 × 10 ⁴	<i>Candida albicans</i>	BDG - 449; <i>C. acbicans</i>

Using broad-range quantitative PCR, fungal 28 S rRNA gene (rDNA) could be detected in 11 ocular samples of ten fungal endophthalmitis cases and one non-infectious case

AH aqueous humor, nt not tested, PPV pars plana vitrectomy, SA systemic antimycotic (oral or intravenous), TA topical antimycotic, VF vitreous fluids

^a Fungal blood test levels of β-D-glucan (BDG: pg/ml), detection of fungal antigens (pg/ml), and conventional fungal cultures

idiopathic uveitis or endophthalmitis patients [7]. However, this PCR examination could not detect other types of fungal infections. Therefore, as the next step, we have developed a novel PCR examination for broad fungi diagnosis. We attempted to detect whole-genomic fungal DNA in humans by PCR amplification of 28 S rDNA [8].

The new assay targets a part of the 28 S rDNA found in *Candida*, *Aspergillus*, *Cryptococcus*, *Mucor*, *Penicillium*, *Pichia*, *Microsporium*, *Trichophyton*, and *Scopulariopsis* [8]. It is assumed that infectious endophthalmitis related to fungal infection may be caused by various human pathogenic fungi, and the ocular infection may indicate various types of endophthalmitis, such as endogenous, post-

Table 2 Summary of risk factors and therapies in fungal endophthalmitis patients

Case no.	Diagnosis	Risk factors	A	B	C	Outcome
24	Endogenous endophthalmitis	IVH, peritoneal catheter	(+)	SA	PPV, SA	Resolved
30	Late postoperative endophthalmitis	Vitrectomy, IOL second implant	(-)	None	PPV, SA	Resolved
77	Endogenous endophthalmitis	Diabetes	(-)	PPV	SA	Resolved
161	Endogenous endophthalmitis	Diabetes	(-)	PPV	Unknown	Unknown
179	Endogenous endophthalmitis	Diabetes, pancreas carcinoma, IVH	(+)	SA, TA	SA, TA	Resolved
231	Endogenous endophthalmitis	Gallbladder carcinoma, IVH	(+)	PPV, SA	SA	Resolved
268	Endogenous endophthalmitis	Triamcinolone subtenon injection	(-)	PPV	SA	Resolved
326	Endogenous endophthalmitis	Aortocoronary bypass, IVH	(+)	PPV, SA	SA, TA	Resolved
355	Late postoperative endophthalmitis	PEA + IOL	(-)	None	TA	Resolved
359	Late postoperative endophthalmitis	PEA + IOL	(+)	PPV, SA	SA	Resolved
455	Primary intraocular lymphom	Lymphoma, steroid use	(-)	Methylprednisolone	Methotrexate	Resolved
461	Endogenous endophthalmitis	Aortocoronary bypass, IVH	(+)	SA	SA	Resolved
490	Endogenous endophthalmitis	Subarachnoid hemorrhage, IVH	(+)	PPV, SA	SA, TA	Resolved

A = presence or absence of antimycotic therapy before PCR examination

B = therapy prior to PCR examination

C = therapy after PCR examination

IVH intravenous hyperalimentation, IOL intraocular lens, PEA phacoemulsification and aspiration, PPV pars plana vitrectomy, SA systemic antimycotic (oral or intravenous)

traumatic, post-operative, and ocular surface infection (e.g., corneal ulcer). Furthermore, real-time PCR assays play an important role among molecular genetic screening methods because of the rapid diagnostic outcome. As shown in the current study, a broad-range real-time PCR assay targeting clinically relevant fungal species in one assay is now available.

In two false-negative cases that were clinically suspected of having fungal endophthalmitis (perhaps *Candida*-associated), our fungal 28 S PCR did not detect any fungal genome in the ocular samples. However, it should be noted that these samples were aqueous humor and not vitreous fluid. If a vitreous sample or a retinal tissue sample had been obtained by biopsy, we might have detected fungal DNA by this PCR method, because endophthalmitis, especially *Candida* spp., often results from hematogenous dissemination. In cases of postoperative endophthalmitis related to fungal infection, the result from an aqueous humor sample as well as a vitreous sample may be reliable. In fact, two aqueous humor samples were used to detect late postoperative endophthalmitis in the current study. Thus, the type of sample that is collected may be very important for an accurate diagnosis. Depending on the exact clinical setting, a vitreous sample likely offers an optimal diagnosis, since the cultures are usually more accurate. An aqueous sample is, obviously, more easily accessible, but the diagnostic power should be quoted only for the type of sample so as not to confuse expectations and dependency on the results. In cases of fungal endophthalmitis in immunocompetent patients, specific additional antimycotic therapy has been shown to be effective in controlling the ocular inflammation [10–12]. In fact, our PCR-negative immunocompetent patients were finally well controlled by the antimycotic treatment.

In conclusion, we developed a novel protocol for the rapid detection of fungal DNA in ocular samples that was based on fungal species that commonly cause eye disorders. This broad-range real-time PCR method can be utilized for rapid diagnosis of patients who have unknown infectious intraocular disorders. For clinicians to be able to identify the type of fungi, we may need to consider the use of sequence analysis. In the near future, we may be able to determine the fungal species via sequence analysis and rapidly diagnose fungal endophthalmitis; then, we will be able to promptly begin appropriate treatment with antimycotic drugs.

Acknowledgments We greatly appreciate the expert technical assistance of Ikuyo Yamamoto and Chizuru Kato.

Funding This work was supported by Comprehensive Research on Disability, Health and Welfare, Health and Labour Sciences Research Grants, Ministry Health, Labour and Welfare, Japan.

Competing interests None.

Contributors MO was the principal investigator, designed and performed experiments, and wrote the manuscript. SS designed and conceptualized the study and drafted and edited the manuscript. KW and NS performed PCR assays. MM designed and conceptualized the study and edited the manuscript.

Data sharing statement No additional data.

Ethics approval Ethics approval was provided by the Institutional Ethics Committee of Tokyo Medical and Dental University.

References

1. Jaeger EE, Carroll NM, Choudhury S, Dunlop AA, Towler HM, Matheson MM, Adamson P, Okhravi N, Lightman S (2000) Rapid detection and identification of *Candida*, *Aspergillus*, and *Fusarium* species in ocular samples using nested PCR. *J Clin Microbiol* 38:2902–2908
2. Hidalgo JA, Alangaden GJ, Elliott D, Akins RA, Puklin J, Abrams G, Vazquez JA (2000) Fungal endophthalmitis diagnosis by detection of *Candida albicans* DNA in intraocular fluid by use of a species-specific polymerase chain reaction assay. *J Infect Dis* 181:1198–1201
3. Bagylakshmi R, Therese KL, Madhavan HN (2007) Application of semi-nested polymerase chain reaction targeting internal transcribed spacer region for rapid detection of panfungal genome directly from ocular specimens. *Indian J Ophthalmol* 55:261–265
4. Khot PD, Fredricks DN (2009) PCR-based diagnosis of human fungal infections. *Expert Rev Anti Infect Ther* 7:1201–1221
5. Kunimoto DY, Das T, Sharma S, Jalali S, Majji AB, Gopinathan U, Athmanathan S, Rao TN (1999) Microbiologic spectrum and susceptibility of isolates: part I. Postoperative endophthalmitis. Endophthalmitis research group. *Am J Ophthalmol* 128:240–242
6. Puliafito CA, Baker AS, Haaf J, Foster CS (1982) Infectious endophthalmitis. Review of 36 cases. *Ophthalmology* 89:921–929
7. Sugita S, Kamoi K, Ogawa M, Watanabe K, Shimizu N, Mochizuki M (2012) Detection of *Candida* & *Aspergillus* species DNA using broad-range real-time PCR for fungal endophthalmitis. *Graefes Arch Clin Exp Ophthalmol* 250:391–398
8. Vollmer T, Störmer M, Kleesiek K, Dreier J (2008) Evaluation of novel broad-range real-time PCR assay for rapid detection of human pathogenic fungi in various clinical specimens. *J Clin Microbiol* 46:1919–1926
9. Sugita S, Shimizu N, Watanabe K, Katayama M, Horie S, Ogawa M, Takase H, Sugamoto Y, Mochizuki M (2011) Diagnosis of bacterial endophthalmitis by broad-range quantitative polymerase chain reaction. *Br J Ophthalmol* 95:345–349
10. Ho PC, Tolentino FI, Baker AS (1984) Successful treatment of exogenous *Aspergillus* endophthalmitis: a case report. *Br J Ophthalmol* 68:412–415
11. Funakoshi Y, Yakushijin K, Matsuoka H, Minami H (2011) Fungal endophthalmitis successfully treated with intravitreal voriconazole injection. *Intern Med* 50:941
12. Biju R, Sushil D, Georgy NK (2009) Successful management of presumed *Candida* endogenous endophthalmitis with oral voriconazole. *Indian J Ophthalmol* 57:306–308

Correlation between multiple *RET* mutations and severity of Hirschsprung's disease

Kunihiro Ishii · Takashi Doi · Ken Inoue ·
Manabu Okawada · Geoffrey J. Lane ·
Atsuyuki Yamataka · Chihiro Akazawa

Published online: 1 November 2012
© Springer-Verlag Berlin Heidelberg 2012

Abstract

Purpose The enteric nervous system (ENS), comprising neurons and glial cells, organized as interconnected ganglia within the gut wall, controls peristalsis and the production of secretions. The RET receptor tyrosine kinase is expressed throughout enteric neurogenesis and is required for normal ENS development. Humans with mutations in the RET locus have Hirschsprung's disease (HSCR), and mice lacking RET exhibit total intestinal aganglionosis. Although a number of mutations with the potential for causing HSCR have been reported, their precise correlation with phenotype and symptom severity in HSCR is not clearly understood. Our study investigates the correlation between mutations in the RET locus and symptom severity in HSCR.

Methods We performed a comprehensive nucleotide analysis of the RET coding region in 18 HSCR patients and 87 controls, performed cellular biological analysis by Western blotting using the expression vector, and analyzed cell proliferation with anti-Ki67 antibody under immunofluorescence confocal microscopy (ICM).

Results We identified three novel mutations, D489N, L769L, and V778D in the RET coding region in our HSCR patients. In the allelic distribution of D489N and L769L, the difference between HSCR patients and controls reached statistical significance ($p = 0.0373$ and $p = 0.0004$, respectively), whereas no statistical difference was observed in the allelic distribution of V778D ($p = 0.1073$). One HSCR patient who died from total colonic aganglionosis had a combination of homozygous mutation of D489N, L769L, and heterozygous mutation of V778D. Western blotting of full mutant RET from this patient showed significantly increased 150kD-band, which corresponds to the immature form compared with wild-type and single mutant RET. ICM showed that overexpression of full mutant RET significantly reduced cellular proliferation in comparison with wild-type and single mutant RET.

Conclusion A combination of mutations in the RET locus may correlate with symptom severity in HSCR as a consequence of reduced cellular proliferation secondary to altered maturation of RET.

Keywords Comprehensive exon nucleotide analysis · Maturation · Proliferation · RET tyrosine-type kinase · Hirschsprung's disease

Introduction

Hirschsprung's disease (HSCR) is a congenital disorder of the enteric nervous system (ENS) and is characterized by the absence of intestinal ganglion cells in myenteric and submucosal plexuses. The length of the aganglionic segment has been used to classify HSCR into short-segment type, rectosigmoid-type, long-segment type, extensive-type, and total-colon aganglionosis. Its incidence is

K. Ishii · C. Akazawa (✉)
Department of Biochemistry and Biophysics, Graduate
School of Health Care Sciences, Tokyo Medical and Dental
University, Yushima, Bunkyo-ku, Tokyo 113-8510, Japan
e-mail: c.akazawa.bb@tmd.ac.jp

T. Doi · M. Okawada · G. J. Lane · A. Yamataka
Department of Pediatric General and Urogenital Surgery,
Juntendo University School of Medicine,
Tokyo 113-8421, Japan

K. Inoue
Department of Mental Retardation and Birth Defect Research,
National Institute of Neuroscience, NCNP,
Tokyo 187-8502, Japan

approximately 1/5,000 human live births, and has a male preponderance of 4:1 [1–3]. There is a spectrum of symptoms, the severity of which can vary widely.

In previous studies, several genes have been reported to be responsible for HSCR in humans; the RET gene [4], the GFR α 1 gene [5], the EDNRB gene [6], the EDN4 gene [6], and the SOX10 gene [7], with the RET proto-oncogene being considered the major candidate gene for causing HSCR [1].

The RET gene encodes the RET receptor tyrosine kinase which is expressed in neural crest-derived cells and the kidneys. RET protein is required for normal ENS development [8] and is broadly divided into two forms. One is a 170 kDa mature glycosylated form, which is localized on cell membranes, and the other is a 150 kDa immature glycosylated form, which is localized in the cytoplasm and endoplasmic reticulum [9]. GFR α is necessary for activation of RET protein in the presence of their ligands such as glial cell line-derived neurotrophic factor (GDNF), neurturin, artemin, and persephin [10]. Activating RET protein triggers the proliferation, differentiation, and survival of ENS cells [11, 12]. When there are mutations in the RET locus, there is abnormal development of the ENS, and mice lacking *Ret* fail to develop ENS and exhibit total intestinal aganglionosis [13, 14]. It has been previously reported that there is deterioration in the maturation of RET protein and its translocation to plasma membranes when there is mutation of the RET extracellular domain [15]. These results suggest that a decrease in matured RET protein on plasma membranes could be a potential cause of HSCR.

Although many studies have provided genetic and molecular evidence for the potential role of RET in HSCR, the precise correlation between molecular phenotype and symptom severity is not clearly understood. To investigate whether a combination of mutations in the candidate locus may contribute to symptom severity in HSCR, we firstly performed a comprehensive nucleotide analysis of common and rare variants of RET obtained from Japanese HSCR patients and constructed an expression vector containing multiple RET mutations identified from a patient with HSCR who died from total colonic aganglionosis, and then performed cellular biological analysis using this expression vector.

Materials and methods

Patients

In this study, 18 Japanese HSCR patients from unrelated families who were treated surgically at Juntendo University Hospital in Japan between 1997 and 2009 were the subjects for this study. A definitive diagnosis of aganglionosis was

obtained from medical records. The control group comprised 87 students from Tokyo Medical and Dental University in Japan. They were unselected, unrelated, age- and sex-mismatched individuals. Informed consent was obtained from all participants. Methodology for collecting medical data and gene analysis were approved by the Research Ethics Committee of the Faculty of Medicine, Juntendo University (approval number 454).

DNA sequencing and mutation analysis

A comprehensive nucleotide analysis of the RET coding region from 18 HSCR patients and 87 controls was performed. Mutation analysis was performed by direct sequencing using an ABI Prism[®]3100 Genetic Analyzer (Life Technologies Japan, Tokyo, Japan). The specific primers used in this study are listed (Table 1).

Cloning

The full-length RET9-D489N, RET9-L769L, RET9-V778D, and RET9-D489N/L769L/V778D were constructed using wild-type human RET9 as a template, using KOD with a mutagenesis system (TOYOBO, Osaka, Japan) according to the manufacturer's instructions. Wild-type human RET9 and mutant type RET9 were inserted into pcDNA3 vector (Life Technologies Japan, Tokyo, Japan) tagged HA. All expression vectors were confirmed by DNA sequencing. The primers used for mutagenesis are listed (Table 2).

Cell culture and transfection

COS7 (African green monkey kidney fibroblast) cells were cultured in Dulbecco's-modified Eagle's medium (DMEM) (Life Technologies Japan, Tokyo, Japan) containing 10 % fetal bovine serum (FBS) (PAA Laboratories, Pasching, Austria), supplemented with 100 U/mL penicillin–streptomycin (Life Technologies Japan, Tokyo, Japan). For RET expression analysis by Western blotting, COS7 cells were plated to a 60 mm diameter dish at a density of 5×10^5 cells per well and transfected with the expression vector using Lipofectamine2000 (Life Technologies Japan, Tokyo, Japan) for 24 h. For proliferation assay by immunostaining, COS7 cells were plated onto the cover glass of a 24 well-plate at a density of 5×10^4 cells per well and transfected in the same way.

Western blotting

Cells were lysed in sodium dodecyl sulphate (SDS) sample buffer by sonication. The lysates were subjected to SDS-polyacrylamide gel electrophoresis, and transferred to

Table 1 Oligonucleotide primers used to amplify RET

Exon	Primers (5'→3')	Product size (bp)
For RET genotyping		
1	F; CAGTGTCCGTCGCGTCC R; ACAGAAAGGCGCTTCTGAAC	290
2	F; GCAGTTCTTTTCTAGCCCGTG R; TTGTCCTGGCTTCTCTCCAG	622
3	F; CCAATCCCGACTGCCTG R; ATGGCTTGTGTCAAGGGC	428
4	F; CTGTGGAGCGGAGGAGG R; ACTAAACCGACCGAGAAACG	453
5	F; TAAGGTCTCTGGTTTTGGGG R; AAGAGCGAGCACCTCATTTTC	328
6	F; TGTGTCTGGGAAGAGGTGTG R; TACTCTGTGCTGGTTGGGC	384
7	F; GGGAATCTCTACCCTCAGGC R; AGGCCAGGCTCCAGAAG	392
8	F; CCTGTCCTTGGGCACTAGC R; CAGGACCCCGTTTCCAC	264
9	F; TCCTCCCTAGAGGGGCAG R; AACTCTGGCTGAAGTGCCTG	287
10	F; TTGGGACACTGCCCTGG R; TGCTGTTGAGACCTCTGTGG	260
11	F; GAGCATA CGCAGCCTGTACC R; GGAAGGCAGCTGGGGAG	383
12	F; CTCCCCTGTCATCCTCACAC R; CTCAGGGTCCCATGCTG	300
13	F; CTGGTATGGTCATGGAAGGG R; GGAGCAGTAGGGAAAGGGAG	272
14	F; CTCCTGGAAGACCCAAGCTG R; GTGGTGGGTCAGGGTGTG	335
15	F; GTGACCGCTGCTGCCTG R; GCTTCCAAGGGCACTG	254
16	F; TCTCCTTACCCTCCTTC R; CCAAGCTGCACAGACGG	228
17	F; GGCTCTGTGAGGGCCAG R; CACAGATGTCCCCTCCCT	246
18	F; CTGTCCTTCTGAGACCTG R; AAATACTGCCCTGGGGT	236
19	F; CCCTGAGGATGGCTTGTTG R; AAAGGTT CAGAGCAGACTTTGG	355

PVDF membranes (GE healthcare Japan, Tokyo, Japan). The membranes were blocked with 5 % fat-free milk in Tris-buffered saline (TBS) containing 0.5 % Tween 20. Membranes were then probed with anti-HA rabbit antibody (Y-11) (Santa Cruz Biotechnology, California, US), which can detect transfected-RET9 proteins at 1:1,000 dilution, and anti-GDNF α goat antibody (C-20) (Santa Cruz Biotechnology, California, US) at 1:1,000 dilution overnight at 4 °C, followed sequentially by reactions with

peroxidase-conjugated anti-rabbit IgG antibody (Sigma), or anti-goat IgG antibody (Sigma). The labelled proteins were developed using ECL Prime Western Blotting Detection (GE Healthcare Japan, Tokyo, Japan) and quantified by software Image J (NIH, Maryland, US) and X-ray radiography.

Proliferation assay

Proliferation was assessed by immunostaining using anti-human Ki67 mouse antibody (BD biosciences, New Jersey, US), which is a marker for cellular proliferation. 24 h after transfection, cells were starvated in DMEM containing 0.1 % FBS (PAA Laboratories) for additional 24 h and subsequently stimulated with FBS and GDNF (30 ng/mL) (R&D systems, Minnesota, US), respectively, for 24 h. Cells were fixed with 4 % paraformaldehyde (PFA) for 15 min, and permialized in 0.1 % saponin in phosphate-buffered saline (PBS) for 20 min. Cells were incubated in a mixture of two primary antibodies: anti-human Ki67 mouse antibody at 1:100 (BD biosciences) dilution and anti-HA rabbit antibody at 1:250 dilution (Y-11) (Santa Cruz Biotechnology) overnight at 4 °C. Cells were then washed in PBS, and incubated in a mixture of two secondary antibodies: Alexa Fluor 594-conjugated goat anti-mouse IgG (Life Technologies Japan, Tokyo, Japan) and Alexa Fluor 488-conjugated goat anti-rabbit IgG (Life Technologies Japan). The stained cells were examined under ICM using software MetaMorph (Molecular Devices Japan, Tokyo, Japan). For the evaluation of proliferation, Ki67-HA double positive cells were scored, based on counting a total of over 5,000 cells, respectively.

Statistical analysis

All numerical data are presented as mean \pm standard error (SE). Differences in allele frequency between the patient and control groups were tested by the Chi-squared test or Fisher's test. Differences between wild-type and mutant-type RET were tested by the unpaired Student's or Welch's *t* test. Differences were regarded as being statistically significant when $p < 0.05$.

Results

Analysis of RET variants in 18 Japanese HSCR patients

We identified several mutations in the RET coding regions in our HSCR patients (Table 3). For the allelic distributions of D489N and L769L, differences between HSCR patients and controls reached statistical significance ($p = 0.0373$ and $p = 0.0004$, respectively), whereas there was no

Table 2 Oligonucleotide primers used for cloning

Mutation	Primers (5'→3')	Product size (bp)
For cloning		
D489N	F; CCAACCAGCAGACCTCTAGGC R; TGGCCACCACCATGTAGTGAAG	RET (3219 bp) + expression vector
L769L	F; CTGCGAGACCTGCTGTCAGAG R; CTCACCTCGGGGAGGCGTTCTC	
V778D	F; GACCTGAAGCAGGTCAACCAC R; GTTGAACTCTGACAGCAGGTC	

Table 3 List of mutations found in our series of HSCR patients

Case no.	Range of aganglionic segment	Position, and amino acid change			
1	Extensive	Exon2 (A45A)	Exon7 (A432A)	Exon13 (L769L)*	Exon13 (V778D)*
2	Rectosigmoid	Exon7 (A432A)*	Exon13 (L769L)*	Exon13 (V778D)*	
3	Rectosigmoid	Exon2 (A45A)	Exon7 (A432A)*	Exon7 (D489N)*	Exon13 (L769L)
4	Extensive	Exon7 (A432A)	Exon13 (L769L)		
5	Total colon	Exon7 (D489N)	Exon13 (L769L)	Exon13 (V778D)*	
6	Rectosigmoid	Exon2 (A45A)*	Exon7 (A432A)*	Exon13 (L769L)*	Exon13 (V778D)*
7	Rectosigmoid	Exon2 (A45A)	Exon7 (A432A)	Exon13 (L769L)	
8	Rectosigmoid	Exon2 (A45A)	Exon7 (A432A)	Exon13 (L769L)	
9	Rectosigmoid	Exon2 (A45A)	Exon7 (A432A)	Exon13 (L769L)	
10	Rectosigmoid	Exon2 (A45A)	Exon7 (A432A)	Exon13 (L769L)	
11	Rectosigmoid	Exon2 (A45A)	Exon7 (A432A)	Exon13 (L769L)	
12	Long	Exon7 (A432A)	Exon13 (L769L)		
13	Rectosigmoid	Exon2 (A45A)	Exon7 (A432A)	Exon13 (L769L)	
14	Rectosigmoid	Exon2 (A45A)*	Exon7 (A432A)*	Exon7 (D489 N)*	Exon13 (L769L)
15	Rectosigmoid	Exon2 (A45A)	Exon7 (A432A)	Exon13 (L769L)	
16	Rectosigmoid	Exon7 (A432A)*	Exon7 (D489N)*	Exon13 (L769L)*	
17	Rectosigmoid	Exon7 (A432A)	Exon7 (D489N)*	Exon13 (L769L)	
18	Rectosigmoid	Exon2 (A45A)	Exon7 (A432A)	Exon13 (L769L)	

* Heterozygous mutation

statistical difference observed for the allelic distribution of V778D ($p = 0.1073$) (Table 4).

One HSCR patient who died from total colonic aganglionosis had a combination of homozygous mutations of both D489N and L769L with an heterozygous mutation of V778D. A brief summary of this patient follows. The male infant was born at term via an elective cesarean section for intrauterine growth retardation and breech presentation, weighing 1.82 kg. He was referred on day 1 of life for further management of bilious vomiting, abdominal distension and delayed passage of meconium. At laparotomy on day 1 of life, a large-caliber change in the diameter of the ileum was identified 85 cm from the Treitz ligament. There were no ganglionic cells identified at the caliber change or in the rectum, and a diagnosis of total colonic aganglionosis was made. An ileostomy was created where normoganglionic cells were identified. He was incidentally found to have severe food allergies leading to failure to

thrive, poor hearing, heterochromia iridis, and a benign sub-mucosal tumor in the oral cavity. A Duhamel procedure was performed some 10 months later, but continuous total parental nutritional support was still required, complicated by several severe central venous catheter infections. He eventually died from multiple organ failure when 25 months old.

Western blotting of RET mutants in COS7 cells

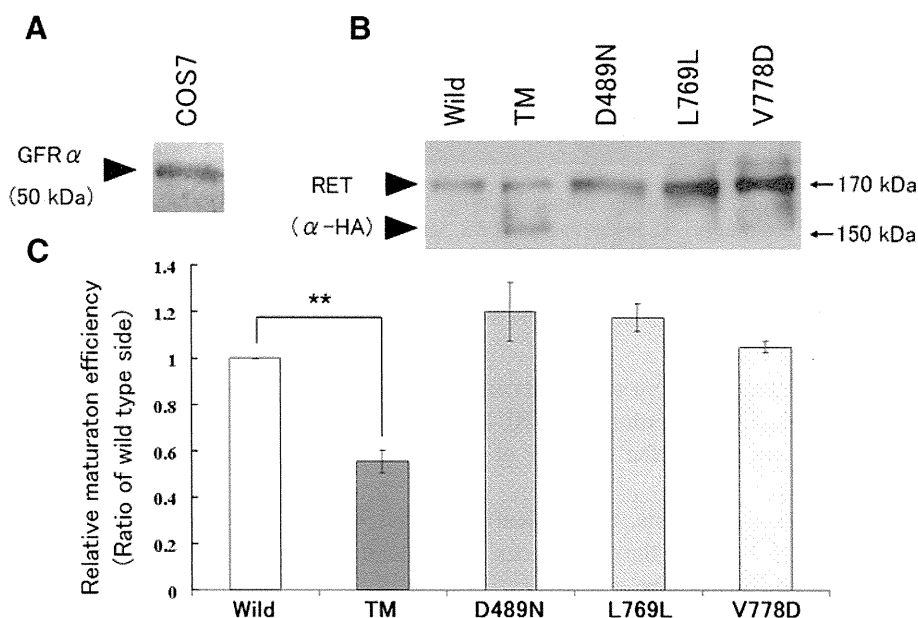
We confirmed that COS7 cells express GFR α using western blotting. (Fig. 1a) We then performed transient transfection using each expression vector, D489N-RET (D489N), L769L-RET (L769L), V778D-RET (V778D) and D489N/L769L/V778D-RET (Triple Mutant RET: TM), in COS7 cells. Protein lysates were prepared 24 h after transfection. Western blotting of the TM RET protein revealed that the 150 kDa immature form increased

Table 4 Allele distribution of RET variants between HSCR patients and controls

Gene and exon	Nucleotide alteration	Codon position and amino acid change	Allele	HSCR (%)	Controls (%)	<i>p</i> value
RET						
Exon7	c1465G>A	D489N	G	30 (83.3 %)	165 (94.8 %)	0.03734
			A	6 (16.7 %)	9 (5.2 %)	
Exon13	c2307T>G	L769L	T	4 (11.1 %)	84 (60.0 %)	0.00035
			G	32 (88.9 %)	90 (40.0 %)	
Exon13	c2333T>A	V778D	T	32 (66.7 %)	166 (90.0 %)	0.10736
			A	4 (33.3 %)	8 (10.0 %)	

Fig. 1 Western blotting of whole COS7 cells lysate and each RET protein; wild type, triple mutant type (TM), D489N mutant type, L769L mutant type, V778D mutant type. **a** The expression of GFR α in COS7 cells is confirmed. **b** Transient expression of wild type and mutant RET proteins.

c Quantitative measurement of the maturation efficiency of each RET protein construct. Differences between wild type and the patient who died with triple mutations were tested using the student's *t* test (***p* < 0.01 versus wild type)



markedly whereas in the other transfections, the 170 kDa mature form predominated (Fig. 1b, c).

Cell Proliferation assay for a combination of three mutant in the RET locus

Proliferation assays were performed under three conditions, RET-stimulation, FBS-supplementation, GDNF-supplementation and serum starvation, in COS7 cells after transient transfection of each expression vector. IMC showed that proliferation of cells expressing TM RET under the condition of FBS-supplementation decreased significantly in comparison with wild-type and single mutant RET (Fig. 2).

Discussion

In this study, we focused on establishing a linkage between multiple mutations in the RET locus and symptom severity in HSCR, then examined the molecular characteristics of

RET proteins in the HSCR patient in our series who had the most severe symptoms. Many studies have investigated candidate genes, their interaction, and gender and ethnic differences in HSCR incidence [1, 16], but symptom severity as an indicator of phenotypic variation secondary to mutations has never been reported. In fact, the phenotype, its incidence, length of aganglionosis, and potential for association with other pathology seems to vary between HSCR patients who carry identical mutations [1].

RET receptor-type tyrosine kinase accounts for the significant protein of both familial and sporadic HSCR, associated with a wide variety of mutations scattered throughout the entire region of coding sequences. Previous studies have shown there is a significant correlation between the allele distributions in mutations A45A and L769L and the length of aganglionosis [17–19]. In our series, a correlation between A45A, L769L, and the severity of aganglionosis was not identified. However, RET L769L variant was carried in all our HSCR patients, and there was a significant correlation between the allelic frequencies due to this variant and the development of HSCR.

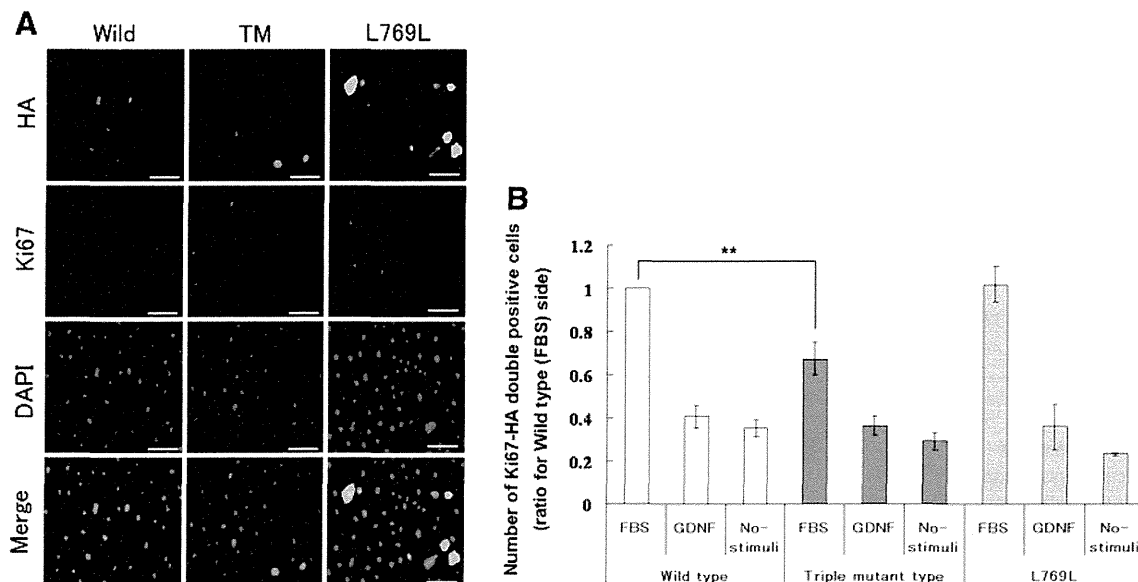


Fig. 2 Proliferation assay using immunostaining with anti-Ki67 under three conditions, RET-stimulation, FBS supplementation, GDNF supplementation, and serum starvation (no-stimuli) in COS7 cells after transient transfection with each expression vector. **a** IMC image under FBS supplementation. **b** Quantitative measurement of

the proliferation of cells expressing each RET protein, wild type, triple mutant type (TM), and L769L mutant type. Differences between wild type and the patient who died with triple mutations were tested using the student's *t* test (***p* < 0.01 versus wild type). Scale bar 100 μ m

Thus, it would appear from our results and previous reports that an L769L silent mutation in the RET locus may have a strong correlation with the severity of symptoms due to aganglionosis.

In this genetic analysis, three silent mutations, A45A, A432A, and L769L, in the RET locus were identified in one of our HSCR patients.

Relating this to the HSCR patient in our series who had such severe symptoms that he passed away, this patient had a combination of triple mutations in the RET locus; D489N and L769L were homozygous, and V778D was heterozygous. When we further investigated the mutations present in this patient, the D489N mutation is in the extracellular domain of RET, and mutations of this domain affect RET processing in the endoplasmic reticulum and disturb the expression of RET on the cell surface [15]. L769L and V778D mutations are in the intracellular domain, and mutations of this domain affect RET tyrosine kinase activity [20]. From these findings, we hypothesized that this patient may have abnormally functioning RET. To test this, we performed cellular biological analyses using the expression vector that contains these triple mutations. Using Western blotting, we found the mature form of RET was significantly decreased only in the patient with the triple RET mutants. Although we did not assess patients with double mutations, our findings would imply that RET maturation or RET transportation is affected detrimentally by the triple mutation combination seen in our patient who died, probably through some mechanism involving failure

of the descent of cell surface RET causing decreased RET kinase activity, resulting in loss of function of RET, although this is purely speculative.

We further examined cellular proliferation which is a characteristic function of RET. The proliferation assay in our patient who died, showed that proliferation of cells expressing triple mutant RET was significantly reduced, indicating that a combination of triple mutations prevented RET from functioning actively. Several groups have reported that there is deterioration in cellular survival and neurite outgrowth when specific mutations decrease RET kinase activity [13, 21]. These findings suggest that a combination of triple mutations in the RET locus may correlate with symptom severity in HSCR, reducing cellular proliferation by altering maturation of RET. A comprehensive analysis in a larger population of HSCR patients with biochemical analysis of molecular mechanisms associated with RET is required to further understand the correlations that may exist between RET mutations and symptom severity in HSCR.

References

1. Amiel J, Sproat-Emison E, Garcia-Barcelo M et al (2008) Hirschsprung disease, associated syndromes and genetics: a review. *J Med Genet* 45:1–14
2. Emison ES, McCallion AS, Kashuk CS et al (2005) A common sex-dependent mutation in a RET enhancer underlies Hirschsprung disease risk. *Nature* 434(7035):857–863